

EVALUATION OF PWR PRESSURE VESSEL FAST NEUTRON FLUENCE BENCHMARKS FROM NUREG/CR-6115 WITH ARES TRANSPORT CODE

by

Liang ZHANG, Bin ZHANG*, Cong LIU, and Yixue CHEN

School of Nuclear Science and Engineering, North China Electric Power University, Beijing, China

Scientific paper

<http://doi.org/10.2298/NTRP1703204Z>

An accurate evaluation of PWR pressure vessel fast neutron fluence is essential to ensure pressure vessel integrity over the design lifetime. The discrete ordinates method is one of the main methods to treat such problems. In this paper, evaluations have been performed for three PWR benchmarks described in NUREG/CR-6115 using ARES transport code. The calculated results were compared to the reference values and a satisfactory agreement was obtained. In addition, the effects of S_N numeric and source distribution modeling for pressure vessel fast neutron fluence calculation are investigated. Based on the fine enough grids adopted, the different spatial and angular discretization introduces derivations less than 3 %, and fix-up for negative scattering source causes no noticeable effects when calculating pressure vessel fast neutron fluence. However, the discrepancy of assembly-wise and pin-wise source modeling for peripheral assemblies reaches ~ 20 %, which indicates that pin-wise modeling for peripheral assemblies is essential. These results provide guidelines for pressure vessel fast neutron fluence calculation and demonstrate that the ARES transport code is capable of performing neutron transport calculations for evaluating PWR pressure vessel fast neutron fluence.

Key words: discrete ordinate, NUREG/CR-6115, reactor pressure vessel, fast neutron fluence, transport calculation

INTRODUCTION

The integrity of pressurized water reactor pressure vessel (RPV) must be guaranteed over the designed lifetime, or even longer when considering the plant life extension in recent years. Radiation embrittlement, primarily caused by fast neutrons, is one of the major factors affecting the integrity of pressure vessel. Therefore, an accurate calculation of fast neutron fluence in the pressure vessel is essential to evaluate material radiation damage. Considering the deep penetration and anisotropy that characterize the fast neutron transport process, discrete ordinates method is one of the methods selected to treat such problems.

The vessel fast neutron fluence benchmark problems described in NUREG/CR-6115 are identified in Guide 1.190 [1] for using in the benchmarking pressure vessel fast neutron fluence prediction methodologies. Traditionally, the 3-D neutron flux distribution is obtained by the synthesis procedure [1, 2], which combines the two-dimensional $R - \theta$, $R - z$ solutions, and one-dimensional R solutions. Also, "bootstrap" is performed where computer-storage limitations prevent a sin-

gle-model representation. The TORSED [3] and TORSET [4] are used for the procedure of bootstrapping, in which the interior boundary neutron flux, picked up from the up-stream region, is used as the boundary source of calculations for the down-stream region. In this paper, a direct 3-D transport calculation based on Cartesian orthogonal structured mesh, is conducted.

Based on the synthesis transport procedure, many analyses have been performed to assess the impact of different issues on the accuracy of fast neutron fluence calculations, including the S_N numeric [5], different multigroup libraries [6], the anisotropy order [7], and the neutron source spectrum [8]. Nowadays, 3-D pressure vessel fast neutron fluence calculation with S_N method is feasible. Therefore, we examine the effect of S_N numeric and source distribution modeling when performing the pressure vessel calculations.

DISCRETE ORDINATES METHOD IN ARES

ARES [9] is a multi-dimensional parallel discrete ordinates neutral particle transport code that uses state-of-the-art solution methods to obtain accurate

* Corresponding author; e-mail: zhangbin@ncepu.edu.cn

solutions to the linear Boltzmann transport equation [10]

$$\int_0^\infty dE \int_{4\pi} d\bar{\Omega} \int_s(\bar{r}, \bar{\Omega}, E) \psi(\bar{r}, \bar{\Omega}, E) - \int_{4\pi} d\bar{\Omega} \int_s(\bar{r}, \bar{\Omega}, E) \psi(\bar{r}, \bar{\Omega}, E) = Q(\bar{r}, \bar{\Omega}, E) \quad (1)$$

There are six independent variables in the steady-state transport equation. The energy variable is discretized in a standard manner to obtain a set of multi-group equations.

The discrete ordinates method is employed to address the discretization of the angular variable. This approximation consists of evaluating the transport equation in distinct angular directions and then, applying a compatible quadrature approximation to angular integrals

$$\phi_g^{nk}(\bar{r}) = \int_{4\pi} \psi_g(\bar{r}, \bar{\Omega}) Y_n^k(\bar{\Omega}) d\bar{\Omega} \quad (2)$$

$$\int_{m=1}^M \psi_g(\bar{r}, \bar{\Omega}_m) Y_n^k(\bar{\Omega}_m) w_m$$

where ϕ_g^{nk} is the neutron angular flux moment of group g , Y_n^k – the neutron angular flux in group g , ψ_g – the spherical harmonic, and $\{\bar{\Omega}_m, w_m\} m = 1, \dots, M$ – the quadrature sets. Currently, ARES provides the level symmetric quadrature sets, the equal weight quadrature sets, the even-odd moment quadrature sets, which are full-symmetric, as well as the Legendre-Chebyshev quadrature sets which are half-symmetric. In addition, a biasing technique based on the Legendre-Chebyshev quadrature sets, called “the angular refinement technique for polar angles”, is developed and implemented in ARES code. From a practical engineering point of view, first collision source method is employed to mitigate ray effects, which appears as unphysical oscillations in the neutron scalar flux and represents the most significant deficiency of the discrete ordinates approximation.

For any given energy group and direction, the transport equation can be reduced to

$$\bar{\Omega}_m \cdot \nabla \psi_{m,g}(\bar{r}) + \Sigma_{t,g}(\bar{r}) \psi_{m,g}(\bar{r}) = Q_{m,g}(\bar{r}) \quad (3)$$

Integrating eq. (3) over a single mesh, we can get the cell-balance equation

$$\frac{|\mu_m|}{\Delta x_i} (\psi_{i,out} - \psi_{i,in}) + \frac{|\eta_m|}{\Delta y_j} (\psi_{j,out} - \psi_{j,in}) + \frac{|\xi_m|}{\Delta z_k} (\psi_{k,out} - \psi_{k,in}) + \Sigma_{t,ijk} \psi_{m,ijk} = Q_{m,ijk} \quad (4)$$

To close eq. (4), the relationship between the cell average neutron fluxes and the face-edge neutron fluxes is introduced

$$\psi_{m,ijk} = \frac{1}{2} \frac{a}{b} \psi_{m,iin} + \frac{1}{2} \frac{a}{c} \psi_{m,iout} + \frac{1}{2} \frac{b}{c} \psi_{m,jin} + \frac{1}{2} \frac{b}{a} \psi_{m,jout} + \frac{1}{2} \frac{c}{a} \psi_{m,kin} + \frac{1}{2} \frac{c}{b} \psi_{m,kout} \quad (5)$$

Several schemes were implemented in ARES to determine the weighting factors a , b and c , including theta weighted (TW), directional theta weighted (DTW), and exponential directional weighted (EDW) [11]. Apart from the cell balance schemes, ARES also employed the linear discontinuous finite element scheme and short characteristic schemes to treat spatial discretization. To avoid negative neutron fluxes in this deep penetration transport calculation, we only consider schemes which produce non-negative neutron fluxes when the source is greater than zero.

RPV FAST NEUTRON FLUENCE CALCULATIONS

Benchmark specification

The PWR calculational benchmark adopts a typical 204 fuel assembly pressurized water reactor core with a power of 2527.73 MW. As depicted in fig. 1, the model includes core region, core barrel, thermal shield, pressure vessel, vessel insulation and an outer concrete biological shield. The details of geometry dimensions and material composition are documented in NUREG/CR-6115. Three surveillance capsules are included in this benchmark: (a) thermal shield capsule, which is located on the outer wall of the thermal shield, (b) pressure vessel capsule, which is located on the inner wall of the vessel, and (c) cavity capsule, which is located at a radius of 320.06 cm and the azimuth of 9.5°. Locations of the first two capsules are illustrated in fig. 1.

Three different types of fuel loadings are evaluated: standard core loading (SCL), low leakage core loading (LLCL), and partial length shield assembly core (PLSA). The SCL model is a typical equilibrium cycle core. The LLCL adopts the same geometry and material information and varies only by the core configuration, in which high burnup fuel assemblies are located on the core periphery to reduce the core leakage. PLSA model employs partial length shield assemblies on the core periphery, in which the fuel rods in the lower sections of the fuel assembly have been replaced with stainless rods for shielding.

Source calculation

The determination of the fission neutron source, which is used as the fixed source in the transport calculations, consists of the absolute source strength with its spatial-energy dependency. The multigroup source distribution can be calculated by

$$S_g(\bar{r}) = \chi_g(\bar{r}) P(\bar{r}) C(\bar{r}) \quad (6)$$

where g is the energy group index, χ_g – the source spectrum, P – the power and C – the power-to-source

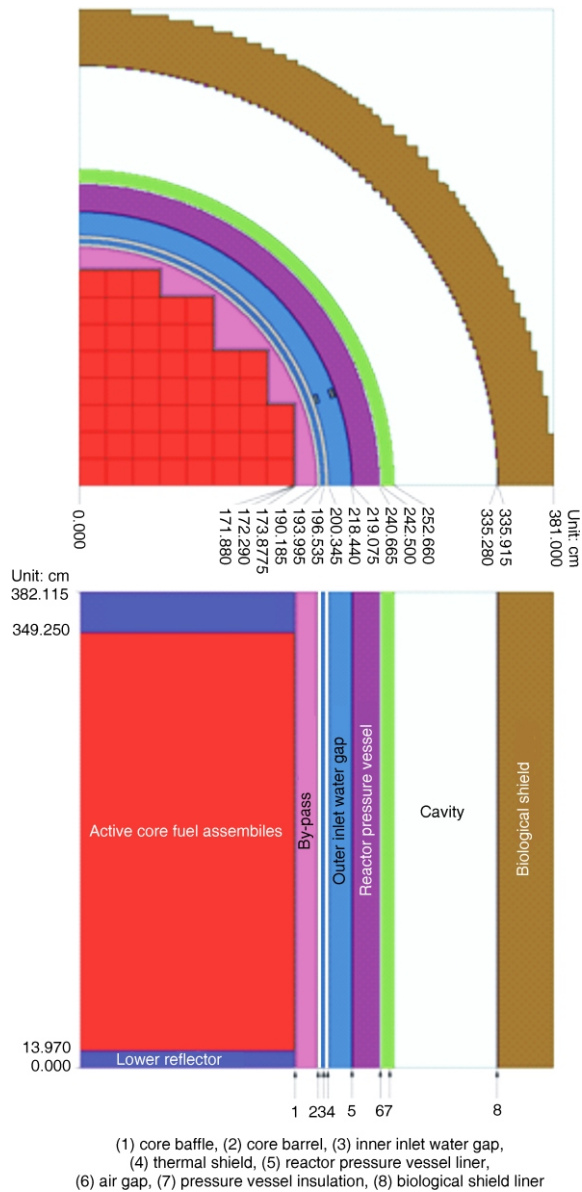


Figure 1. Geometry configuration of the pressurized water reactor model

conversion factor. The power distribution $P(\vec{r})$ can be determined by the relative assembly power, the axial power distributions and the total power, which are all provided in NUREG/CR-6115.

For a single isotope, the source spectrum is the fission spectrum and the power-to-source conversion factor can be evaluated by

$$C = \frac{\nu}{E_r} \quad (7)$$

where ν denotes the average number of neutrons emitted per fission and E_r denotes the recoverable energy released per fission.

Considering the different isotopic fission fractions within different assemblies, the determination of $\chi_g(\vec{r})$ and $C(\vec{r})$ must account for the fact that changes in isotopic fission fractions with fuel exposure result in variations in the fission spectra, the number of neutrons emitted per fission and the recoverable energy

released per fission. Based on fission fraction averaging, the equivalent $C(\vec{r})$ and $\chi_g(\vec{r})$ can be given by

$$C(\vec{r}) = \frac{F^j(\vec{r})\nu^j}{F^j(\vec{r})E_r^j} \quad (8)$$

and

$$\chi_g(\vec{r}) = \frac{F^j(\vec{r})\chi_g^j}{F^j(\vec{r})} \quad (9)$$

where $F^j(\vec{r})$ refers to the fission fraction of isotope j , which has dependency upon the fuel exposure at location \vec{r} . For this benchmark, the fission fraction by isotope as function of exposure is available in NUREG/CR-6115.

In this paper, the spatial dependency of parameters $C(\vec{r})$ and $\chi_g(\vec{r})$ is addressed by averaging over each assembly. Also, the power distribution $P(\vec{r})$ is averaged over each assembly for interior assemblies and over each fuel pin for outer three periphery assemblies.

Transport calculation

After determining the source distribution, the transport of neutrons from the core to the location of interest in the pressure vessel, is simulated by ARES transport code.

A multi-group neutron cross section library is prepared based on the FENDL-3.0 library for mixtures, corresponding to each zones in the models. To evaluate fast neutron fluence, the Vitamin-J energy structure, which contains 104 groups from ~0.1 MeV to 19.64 MeV, is employed. And P-5 Legendre expansion of scattering cross-section is used. Because of the truncated Legendre expansion, a negative scattering source may be obtained for some directions. To guarantee the positivity of the source, the negative total source is set to zero as soon as it appeared.

To avoid negative neutron fluxes and obtain reliable results, EDW spatial differencing scheme is adopted. And a Cartesian structured grid containing 520 322 58 meshes is constructed by GGTM [12]. For angular discretization, we employ Legendre-Chebyshev quadrature set, which is derived by setting the polar angles equal to the roots of the Legendre polynomial and the azimuthal angles equal to the roots of Chebyshev polynomials. A point-wise neutron flux convergence of 10^{-4} is used.

In addition, the effects of different spatial discretization, different order of quadrature sets, the fix-up for the negative scattering source and different homogenization levels of source distribution modeling are investigated in this paper.

RESULTS AND DISCUSSION

In this section, ARES calculated results including fast neutron fluence rate, fast neutron spectrum and do-

simetry reaction rates are presented and compared with reference values documented in NUREG/CR-6115.

Fast neutron fluence rate is calculated at a certain radius as a function of azimuth. To reduce the amount of information, root mean square (RMS) of the relative error was selected to assess the overall accuracy

$$RMS = \sqrt{\frac{1}{N} \sum_{i=1}^N \left(\frac{\phi_{i,cal} - \phi_{i,ref}}{\phi_{i,ref}} \right)^2} \quad (10)$$

where N is the number of locations at a certain radius and ϕ_{cal} and ϕ_{ref} denotes calculated neutron flux and corresponding reference values, respectively.

Table 1 summarizes the RMS error of fast neutron fluence for SCL model. Overall, the maximum RMS errors at these locations are about 23 % compared to S_N reference values and 13 % compared to MCNP results, respectively. These disagreements are expected when considering the following aspects:

(a) the fact that the reference results are based on synthesis method and ARES conduct a direct 3-D transport calculation. The reference calculations were performed for a radial $R-\theta$ plane, an axial plane and a 1-D R geometry. Also, a two-step “bootstrap” fashion is used in $R-\theta$ calculation,

(b) the differences between the FENDL-3.0 library adopted in ARES and BUGLE-93 library employed in reference.

As for detailed differences along the azimuth angle, we compare the fast neutron fluence rate ($E > 1.0$ MeV) at the inner wall of the vessel as a function of azimuth angle and plot the SCL/LLCL results at axial peak location in

Table 1. RMS error of fast neutron fluence

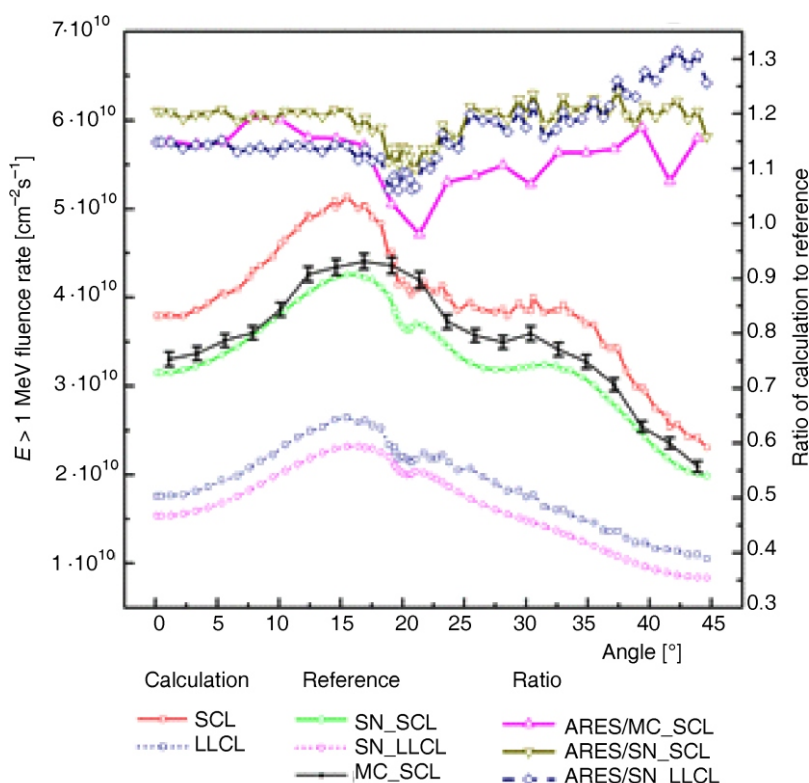
Position		RMS error of fast neutron fluence [%]		
		$E > 1.0$ MeV	$E > 0.1$ MeV	$E > 1.0$ MeV
Axial	PV 0T	18.7268	22.4122	13.2808
Peak	PV 1/4T	18.2676	19.4015	13.7017
Location	PV 1/2T	21.1745	22.5885	/
Lower	PV 0T	15.9070	19.0895	9.3166
Weld	PV 1/4T	15.4313	15.9136	/
Location	PV 1/2T	18.1638	18.7407	/
Down comer		19.6728	23.0537	/
Reference		S_N results		MCNP result

fig. 2 and SCL/PLSA results at lower weld location in fig. 3. As expected, the LLCL core loading significantly reduces the vessel inner-wall fast neutron fluence, and the PLSA core design distinctly reduces the fast neutron fluence at the lower weld location from 0 to ~30 azimuth angle. For most points selected, the calculation to reference ratios lie in the scope from 1.1 to 1.3. The ratios exhibit a noticeable decrease near 20 degree due to the fact that separate capsule models were performed in NUREG/CR-6115.

With the purpose of evaluating calculated energy-dependent neutron fluxes, we compare the fast neutron spectrum at three capsule locations. As illustrated in fig. 4, good agreement is obtained above 1 MeV, while higher results are obtained from 0.1 MeV to 1 MeV. These differences increases as the capsule location is moving farther from the core center, which may be caused by the different cross-section used in our calculation.

In order to investigate the impact of the S_N numeric, we selected the base case of SCL model, which

Figure 2. Comparison of fast neutron fluence rate on model SCL/LLCL



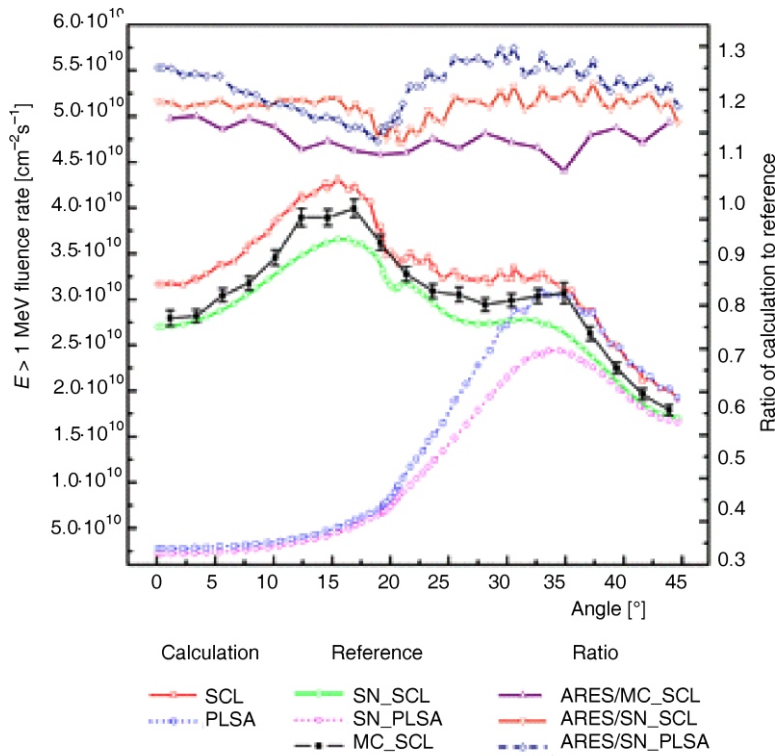


Figure 3. Comparison of fast neutron fluence rate for model SCL/PLSA

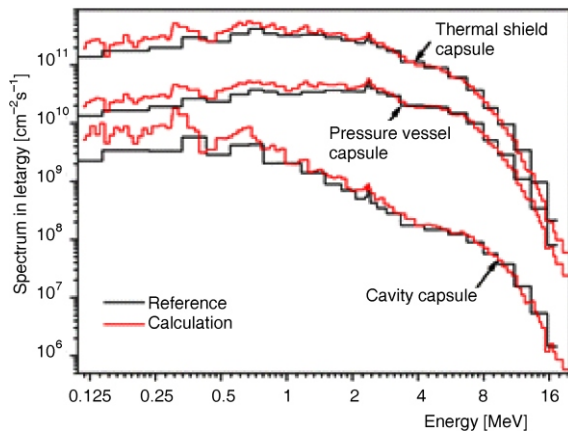


Figure 4. Comparison of fast neutron spectrum at different capsule positions

uses the Legendre-Chebyshev S_{16} quadrature set, EDW spatial discretization, and negative source set-zero fix-up. The effects of the changes in numeric were examined individually as follows:

- (a) spatial discretization (DZ, TW, DTW),
- (b) angular discretization (S_8 , S_{24} , S_{32} of Legendre-Chebyshev quadrature sets), and
- (c) no scattering source fix-up.

The results are depicted in fig. 5. The TW($\theta = 0.0$) spatial discretization causes $\sim 2.5\%$ effect, while other schemes present $\sim 1\%$ effect based on the fine enough grids. Few effects are observed when increasing the order of quadrature sets from S_{16} , except for the cavity position, in which the calculated results are influenced by neutron streaming effects in the low-density materials. The effect of negative scatter-

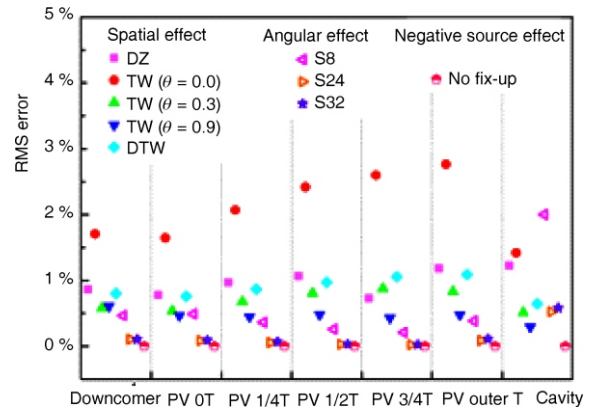


Figure 5. Effects of S_N numeric on fast neutron fluence calculation

ing source fix-up can be negligible when calculating fast neutron fluence.

In order to investigate the effect of source strength distribution, calculations with different source homogenization levels were performed. Figure 6 shows assembly-wise power distribution and peripheral assemblies pin-wise power distribution, respectively. Compared to the results obtained with pin-wise source distribution in three peripheral assembly layers, the deviation of different layers of pin-wise source distribution is listed in tab. 2. The results indicate that the strong radial power gradients in the peripheral assemblies should not be neglected because the peripheral assembly contributes most to the vessel fast neutron fluence.

Table 3 presents a comparison of ARES calculated reaction rates and NUREG reference values for

Figure 6. (a) Assembly-wise and (b) pin-wise power distribution for peripheral assemblies

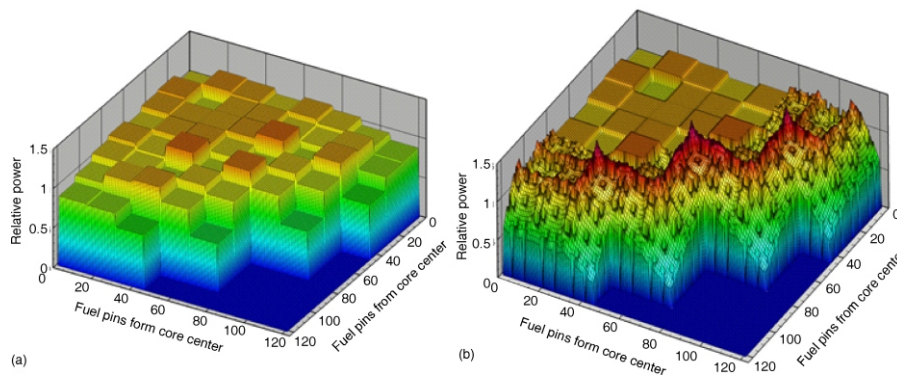


Table 2. Effect of source distribution modeling

Position	Number of peripheral assembly layers with pin-wise source distribution		
	2	1	0
Downcomer	0.1284 %	2.2606 %	22.3161 %
PV OT	0.1303 %	2.1511 %	21.0520 %
PV 1/4T	0.1137 %	2.0805 %	20.8615 %
PV 1/2T	0.1213 %	2.0511 %	20.6989 %
PV 3/4T	0.1125 %	1.9846 %	20.5755 %
PV Outer T	0.0946 %	1.8239 %	20.4069 %
Cavity	0.0520 %	1.3729 %	19.9704 %

SCL and LLCL models. For all the reaction rates considered, an overestimate of 10 %~30 % was obtained, except for $^{65}\text{Cu} (n, 2n)$ reaction. It is noteworthy that the response range of $^{65}\text{Cu} (n, 2n)$ is higher than 10.5 MeV. Above 10.5 MeV, there are 15 groups in Vitamin-J energy structure while only 3 groups are employed in reference calculation. The significantly different energy structure causes the higher deviation. Overall, the calculated results lie in a satisfactory agreement with the reference values.

CONCLUSION

In this paper, the pressure vessel fast neutron fluence prediction capability of ARES transport code is verified by evaluating PWR pressure vessel fast

neutron fluence benchmarks from NUREG/CR-6115. Considering the different libraries employed and different transport calculation methods conducted, the calculated fast neutron fluence at the inner wall of pressure vessel lies in satisfactory agreement with the reference values documented in NUREG/CR-6115.

Additionally, the effects of S_N numeric and source modeling were investigated. Based on the fine enough grids adopted, the different spatial discretization schemes introduces a deviation less than 3 %, and different order of quadrature sets give a discrepancy less than 1 % except for cavity region, while negative source fix-up causes no noticeable effects. However, the accurate calculation and modeling of the source distribution, especially for the peripheral assembly, is essential to calculate the pressure vessel fast neutron fluence with high accuracy.

All these results demonstrate that the ARES transport code is capable of performing neutron transport calculations for evaluating PWR pressure vessel fast neutron fluence.

ACKNOWLEDGEMENT

This work was supported by National Natural Science Foundation of China (11505059, 11575061) and the Fundamental Research Funds for the Central Universities (2016MS59)

Table 3. Reaction rates comparison results for capsules in SCL/LLCL models

Detector material	SCL			LLCL		
	Thermal shield capsule	Pressure vessel capsule	Cavity capsule	Thermal shield capsule	Pressure vessel capsule	Cavity capsule
$^{27}\text{Al}(n, \gamma)$	1.2014	1.1263	1.2233	1.1943	1.1157	1.2415
$^{32}\text{S}(n, p)$	1.1639	1.1175	1.3241	1.1136	1.0780	1.2955
$^{46}\text{Ti}(n, p)$	1.1168	1.0787	1.2041	1.0976	1.0596	1.2068
$^{54}\text{Fe}(n, p)$	1.1342	1.0953	1.2629	1.0897	1.0591	1.2399
$^{56}\text{Fe}(n, p)$	1.2508	1.1812	1.2893	1.2379	1.1652	1.3016
$^{58}\text{Ni}(n, p)$	1.1406	1.1032	1.2875	1.0930	1.0654	1.2597
$^{63}\text{Cu}(n, \alpha)$	1.1789	1.1172	1.2196	1.1646	1.1008	1.2296
$^{65}\text{Cu}(n, 2n)$	1.2827	0.1228*	1.3958	1.3286	1.2652	1.4749
Average	1.1811	1.1171	1.2758	1.1649	1.1136	1.2812

*Reference values documented in NUREG/CR-6115 are suspected

AUTHORS' CONTRIBUTIONS

Under the Y. Chen's guidance, L. Zhang and B. Zhang constructed the benchmark models and calculated the fast neutron fluence results with ARES transport code. C. Liu calculated the Legendre-Chebyshev quadrature sets. All the authors contributed to the development of ARES transport code, analyzed and discussed the results. The manuscript was prepared and written by L. Zhang.

REFERENCES

- [1] ***, U. S. Nuclear Regulatory Commission, Regulatory Guide 1.190, Computational and Dosimetry Methods for Determining Pressure Vessel Neutron Fluence, U.S. Nuclear Regulatory Commission, Washington, D. C., USA, 2001
- [2] Carew, J. F., *et al.*, PWR and BWR Pressure Vessel Fluence Calculation Benchmark Problems and Solutions, NUREG/CR-6115, Washington, D. C., USA, 2001
- [3] Rhoades, W. A., The TORSSED Method for Construction of TORT Boundary Sources from External DORT Flux Files, ORNL/TM-12359, Oak Ridge National Laboratory, Tenn., USA, 1993
- [4] Azmy, Y. Y., Applications of the Discrete Ordinates of Oak Ridge System (DOORSE) Package to Nuclear Engineering Problems, XV SNM Annual Meeting and XXII SMSR Annual Meeting, Cancun, Q. R., Mexico, 2004
- [5] Petrović, B. G., Haghghat, A., Effects of S_N Method Numerics on Pressure Vessel Neutron Fluence Calculations, *Nuclear Science and Engineering*, 122 (1996), 2, pp. 167-193
- [6] Haghghat, A., Veerasingam, R., Transport Analysis of Several Cross-Section Libraries Used for Reactor Pressure Vessel Fluence Calculations, *Nuclear Technology*, 101 (1993), 2, pp. 237-243
- [7] Petrović, B. G., *et al.*, Evaluation of Anisotropy Effects in Pressure Vessel Fluence Calculations Using BUGLE-93 Library, *Transactions of the American Nuclear Society*, 71 (1994), pp. 388-391
- [8] Haghghat, A., Mahgerefteh, M., Evaluation of the Uncertainties in the Source Distribution for Pressure Vessel Neutron Fluence Calculations, *Nuclear Technology*, 109 (1995), 1, pp. 54-75
- [9] Chen, Y., *et al.*, ARES: A Parallel Discrete Ordinates Transport Code for Radiation Shielding Applications and Reactor Physics Analysis, *Science and Technology of Nuclear Installations*, 2017 (2017), ID 2596727
- [10] Lewis, E. E., Jr. Miller, W. F., Computational Methods of Neutron Transport, American Nuclear Society, La Grange Park, Ill., USA, 1993
- [11] Sjoden, G. E., PENTRAN: A Parallel 3-D S_N Transport Code with Complete Phase Space Decomposition, Adaptive Differencing and Iterative Solution Methods, Ph. D. thesis, The Pennsylvania State University, Penn., USA, 1997
- [12] Orsi, R., BOT3P: Bologna Radiation Transport Analysis Pre-Post-Processors Version 4.0, *Nuclear Science and Engineering*, 150 (2005), 3, pp. 368-373

Received on March 27, 2017

Accepted on July 12, 2017

Љјанг ЦАНГ, Бин ЦАНГ, Цунг ЉУ, Јисјје ЧЕН

**ОЦЕНА ARES ТРАНСПОРТНИМ КОДОМ РЕФЕРЕНТНИХ
ФЛУЕНСА БРЗИХ НЕУТРОНА У СУДУ ПОД ПРИТИСКОМ PWR
РЕАКТОРА ИЗ ВОДИЧА NUREG/CR-6115**

Тачна процена флуенса брзих неутрона у суду под притиском PWR реактора од суштинског је значаја за осигурање интегритета суда током пројекторваног животног века. Метода дискретних ордината једна је од главних метода за третирање таквих проблема. У овом раду извршене су оцене за три PRW референтна случаја описана у водичу NUREG/CR-6115, користећи се ARES транспортним кодом. Израчунати резултати упоређени су са референтним вредностима и добијено је задовољавајуће слагање. Поред тога, испитани су ефекти нумеричких модела и моделовања расподеле извора у суду под притиском на флуенс брзих неутрона. На основу усвојених довољно финих мрежа, различита просторна и угона дискретизација увода деривације мање од 3 %, а поправљање негативног изовра расејања не узрокује значајне ефекте при израчунавању флуенса брзих неутрона у суду под притиском. Међутим, неусаглашеност модела извора, склопа и штапа, за периферне склопове достиже 20 %, што укидује на то да је модел штапа периферних склопова од суштинског значаја. Ови резултати обезбеђују смернице за израчунавање флуенса брзих неутрона суда под притиском и показују да је ARES транспортни код способан за извођење прорачуна транспорта неутрона ради процене флуенса брзих неутрона PWR суда под притиском.

Кључне речи: дискретна одринаја, NUREG/CR-6115, реакторски суд под притиском, флуенс брзих неутрона, транспортни прорачун